HHS Public Access

Author manuscript

Biomaterials. Author manuscript; available in PMC 2015 July 15.

Published in final edited form as:

Biomaterials. 2013 December ; 34(38): 9969–9979. doi:10.1016/j.biomaterials.2013.09.020.

Comparison of Photopolymerizable Thiol-ene PEG and Acrylate-Based PEG Hydrogels for Cartilage Development

Justine J. Roberts[1,2] and **Stephanie J. Bryant**[1,2,3,*]

[1]Department of Chemical and Biological Engineering, University of Colorado, Boulder, CO 80303

[2]BioFrontiers Institute, University of Colorado, Boulder, CO 80303

[3]Material Science and Engineering Program, University of Colorado, Boulder, CO 80303

Abstract

When designing hydrogels for tissue regeneration, differences in polymerization mechanism and network structure have the potential to impact cellular behavior. Poly(ethylene glycol) hydrogels were formed by free-radical photopolymerization of acrylates (chain-growth) or thiol-norbornenes (step-growth) to investigate the impact of hydrogel system (polymerization mechanism and network structure) on the development of engineered tissue. Bovine chondrocytes were encapsulated in hydrogels and cultured under free swelling or dynamic compressive loading. In the acrylate system immediately after encapsulation chondrocytes exhibited high levels of intracellular ROS concomitant with a reduction in hydrogel compressive modulus and higher variability in cell deformation upon compressive strain; findings that were not observed in the thiol-norbornene system. Long-term the quantity of sulfated glycosaminoglycans and total collagen was greater in the acrylate system, but the quality resembled that of hypertrophic cartilage with positive staining for aggrecan, collagens I, II, and X and collagen catabolism. The thiol-norbornene system led to hyaline-like cartilage production especially under mechanical loading with positive staining for aggrecan and collagen II and minimal staining for collagens I and X and collagen catabolism. Findings from this study confirm that the polymerization mechanism and network structure have long-term effects on the quality of engineered cartilage, especially under mechanical loading.

Introduction

Free-radical polymerizations have emerged as a promising strategy to encapsulate cells in hydrogels owing to their fast gelation times occurring at physiological temperature and pH [1–3]. Photopolymerization offers additional spatial and temporal control over the reaction allowing for *in situ* polymerization of materials with well-defined structures [4, 5]. Numerous natural [6–9] and synthetic [10–14] polymers have been functionalized with vinyl groups to form hydrophilic macromolecular monomers, or macromers, that can be

*corresponding author: Phone: (303) 735-6714, Fax: (303) 492-4341, Stephanie.Bryant@Colorado.EDU.

polymerized via free-radical polymerization to form hydrogels. To this end, a wide range of macromer chemistries and hydrogel properties can be achieved and subsequently tailored to a particular cell type. Furthermore, reaction conditions for free-radical photopolymerization have been identified which enable encapsulation of cells while maintaining high viability [11, 15, 16], making photopolymerization promising for tissue engineering and *in vivo* cell delivery. However, the choice of polymerization mechanism (e.g., the type of polymerizable moiety) and resulting network structure could have a significant effect on cell function and long-term tissue development.

Depending on the polymerizable moiety chosen for free-radical mediated polymerization, multi-functional macromers can undergo chain or step-growth polymerization [11, 17, 18]. These polymerization mechanisms can be initiated under similar conditions (e.g., photoinitiation involving the same photoinitiator, wavelength, and light intensity). However distinct differences arise during polymerization especially when oxygen is present. The primary differences include the type of propagating radical and its reactivity with oxygen. Molecular oxygen acts as a radical scavenger resulting in the formation of reactive oxygen species (ROS) such as peroxy radicals [19, 20]. Free-radical polymerization of chain-growth (meth)acrylates are notorious for being inhibited by oxygen leading to an accumulation of ROS. On the other hand, free-radical step-growth polymerization between a thiol and vinyl group (referred to as ‘ene’) can be propagated by ROS and thus consume ROS [21]. Extracellular ROS is known to generate oxidative stress in cells [22, 23] and has been linked to inhibition of tissue synthesis and upregulation of tissue degrading enzymes [24, 25]. The differences in reactivity with oxygen between the thiol-ene and acrylate systems may therefore differentially affect cells during encapsulation.

Another distinct difference that arises, depending on the polymerization mechanism, is polymer network structure. When radical mediated chain-growth polymerizations of water soluble (meth)acrylate macromers are performed in aqueous solutions, polydisperse and hydrophobic poly(meth)acrylate kinetic chains are formed. These kinetic chains lead to heterogeneities in crosslink density and therefore network structure [17, 26]. In contrast, thiol-ene polymerizations proceed by an orthogonal, step-growth mechanism where one thiol reacts with one ene leading to a more homogenous distribution in crosslinks [11, 17]. For applications in tissue engineering where mechanical forces are prevalent, differences in network structure may impact how stresses and strains are translated through the hydrogel [27] into local mechanical cues perceived by the cells.

This study therefore aimed to determine whether differences arising between free-radical polymerized hydrogels formed by two distinct mechanisms, acrylates through chain-growth and thiol-enes through step-growth, have an effect on encapsulated cells for cartilage tissue engineering. Specifically, this study posed three research questions. 1) Does photopolymerization by chain-growth and step-growth differentially affect cells during encapsulation in hydrogels? 2) Does the network structure formed by chain-growth and step-growth polymerizations differentially translate mechanical cues to encapsulated cells in the form of cell deformation? 3) Does the combination of polymerization mechanism and network structure have long-term effects on tissue production and composition when cells are encapsulated in hydrogels and subjected to mechanical loading? To address these

questions, synthetic macromers based on poly(ethylene glycol) (PEG) were employed, which were functionalized to polymerize by radical mediated chain-growth (e.g., PEG diacrylate [28]) or step-growth (e.g., PEG tetranorbornene and PEG dithiol [11]) mechanisms and which form stable or degrading hydrogels [11, 12, 17]. Cartilage cells (i.e., chondrocytes) were investigated because chondrocytes maintain their phenotype when encapsulated in synthetic hydrogels [29] and mechanical forces are critical to their function [30, 31].

Materials and Methods

Macromer Synthesis

Poly(ethylene glycol) diacrylate (PEGDA, 4600 Da) and hydrolytically degradable oligo(lactic acid)-*b*-PEG-*b*-oligo(lactic acid) diacrylate (PEG-LA-DA, 4600 Da, 1.3 lactic acid per side) were synthesized as described previously [13]. PEG-tetranorbornene (PEGTNB) was synthesized by reacting 4arm-PEG-NH_2 (5000 Da, JenKemUSA) with 4 molar excess 5-norbornene-2-carboxylic acid (Sigma) in dimethylformamide in the presence of 2 molar excess 2-(1H-7-Azabenzotriazol-1-yl)-1,1,3,3-tetramethyl uronium hexafluorophosphate methanaminium (HATU, AKSci) and 2 molar excess N,N-diisopropylethylamine (DIEA, Sigma). PEGTNB was precipitated in ice-cold diethyl ether, dialyzed against diH_2O, sterile filtered and the final product was collected after lyophilization. Hydrolytically degradable PEG-tetranorbornene (degPEGTNB) was synthesized as described previously [11]. PEG-dithiol (PEGDSH) was purchased (3400 Da, LaysanBio). Functionalization of PEG with acrylate or norbornene was determined using ^1H nuclear magnetic resonance (NMR) imaging. Percent substitution was determined by comparing the area under the carbon-carbon double bond peak associated with the acrylate (5.8, 6.2, 6.4ppm) or the area under the alkene peak associated with the norbornene (~6 ppm) to the area under the peaks of the methyl groups in PEG (~3.6 ppm). Acrylate substitution (two per PEG molecule) was confirmed to be 70–100%. Norbornene substitution (four per PEG molecule) was confirmed to be 95–100%.

Cell Isolation, Encapsulation and Viability

Full-depth articular cartilage was harvested from the patellar-femoral groove of up to two 1–3 week-old calves (Research 87) within 24 h of slaughter. The tissue was digested in 500 units/mL collagenase type II (Worthington Biochemical) following previously published protocols [32]. Freshly isolated cells were >85% viable determined by trypan blue exclusion. PEGDA, PEG-LA-DA, PEGTNB:PEGDSH (1 ene: 1 thiol), degPEGTNB:PEGDSH (1 ene:1 thiol) were dissolved in PBS to final concentrations of 6–11% (w/w) with 0.05% (w/w) photoinitiator I2959 (1-[4-(2-hydroxyethoxy)-phenyl]-2-hydroxy-2-methyl-1-propane-1-one) (Ciba-Geigy). Macromer concentration was varied such that the tangent compressive modulus of the hydrogels in their swollen state was similar for the two different hydrogel systems. Freshly isolated chondrocytes were suspended in sterile macromer/photoinitiator solutions at a final concentration of 50×10^6 chondrocytes/mL. A 50 μL volume of cell suspension was polymerized using 352 nm light at 6 mW/cm^2 for 10 min into cylindrical constructs (~5 mm in diameter and ~2.5 mm in height). Cell-hydrogel constructs were incubated at 37°C and 5% CO_2 in chondrocyte medium (DMEM

supplemented with 10% FBS (v/v), 0.04mM L-proline, 50 mg/L L-ascorbic acid, 10 mmol HEPES per L, 0.1 mol Minimum Essential Medium with nonessential amino acids/L, 1% penicillin/streptomycin, 0.5 μg/mL fungizone, and 20 μg/mL gentamicin). Cell viability of the encapsulated cells was determined by a membrane integrity assay (Live/Dead® Cell Viability Assay (Invitrogen)), which stains live cells green and dead cells red, and imaged on a Zeiss LSM 5 Pascal confocal microscope.

Cell Culture and Mechanical Loading

Hydrogels were cultured under free swelling conditions or in custom bioreactors [32] at 37°C and 5% CO_2 for up to 46 days. Culture medium was replaced every 2 to 3 days. After 24 hours of free swelling culture (referred to as day 0), hydrogels were placed into the bioreactor between permeable platens made of Porex® HDPE (40–70 μm) and subjected to unconfined compressive loading applied intermittently from 0 to 10% strain in a sinusoidal waveform at a frequency of 1 Hz (8 cycles/day of 0.5 h on, 1.5 h off, followed by 8 h off).

Hydrogel Degradation

Acellular PEG-LA-DA and degPEGTNB:PEGDSH were photopolymerized using identical sterile conditions as described above. Each hydrogel was weighed immediately after polymerization to determine initial polymer mass (m_{pi}), then placed in chondrocyte medium, which was replaced every 2 to 3 days, and in an incubator at 37°C and 5% CO_2. At specified time points, hydrogels were lyophilized and their dry polymer mass (m_p) determined. Percent mass loss was determined by

$$\text{Mass Loss} = \left(\frac{m_{pi} - m_{pi}}{m_{pi}} \right) \times 100\%$$

Intracellular Reactive Oxygen Species (ROS)

Intracellular ROS was qualitatively assessed immediately after polymerization in PEGDA and PEGTNB:PEGDSH constructs. In brief, chondrocytes in suspension were incubated with carboxy-H_2DFFDA (carboxy-2,7-difluorodihydrofluorescein diacetate, Invitrogen) for 20 min, rinsed in PBS via centrifugation, and encapsulated in PEG hydrogels as described above. Immediately post-encapsulation, hydrogels were imaged on a Zeiss LSM 5 Pascal confocal microscope. A sample size of 3 was used.

Mechanical Testing

Shear—*In situ* dynamic photorheology [33] was used to measure evolution of shear storage (G′) and loss (G″) moduli during photopolymerization of PEGDA and PEGTNB:PEGDSH in the absence or presence chondrocytes at 50 million cells/mL (n=4 per condition). A rheometer (Ares 4400, TA Instruments) was modified to enable simultaneous irradiation (320–390nm; 6mW/cm^2) of the sample and moduli measurements during a dynamic time sweep with a frequency of 10 Hz and strain of 10% [15]. Plate diameter was 20 mm and plate separation was 50 μm.

Compression—Tangent compressive modulus was determined for chondrocyte-laden constructs at specified time points during culture under unconfined compression (MTS Synergie 100) applied at a constant strain rate (0.5 mm/min).

Cell Deformation

Chondrocyte-laden PEGDA and PEGTNB:PEGDSH constructs with similar tangent moduli were cultured under free swelling conditions in chondrocyte medium for 18 hours. Cell-laden hydrogels were treated with 2μM calcein-AM to stain the cytosol green and then placed in a custom-built straining device and imaged on an inverted confocal microscope [31]. A static compressive strain was applied to the hydrogel at 0% strain and then at 20% strain. Fifty cells per hydrogel (n=4) per strain condition were imaged. The diameter at full-width half-maximum height of each cell was measured along the axis parallel (x) and perpendicular (y) to the applied strain using NIH ImageJ software. Cell deformation was assessed by a diameter ratio (x/y).

Biochemical Assays

At specified time points, constructs were lyophilized, weighed (dry construct weight), homogenized and then digested in an enzyme solution [100mM sodium phosphate buffer, 10mM Na_2EDTA, 10mM L-cysteine, 0.125 mg/ml papain (Worthington)] for 16 h at 60°C. DNA content was measured using Hoechst 33258 (Polysciences), and converted to number of chondrocytes assuming 7.7 pg of DNA per cell [34]. Sulfated glycosaminoglycan (sGAG) content was determined using dimethylmethylene blue (DMMB) dye [35]. Total collagen content was determined by hydroxyproline [36], which is estimated as ~10% of collagen [37]. A sample size of 8 was used for the experiments with non-degradable hydrogels. A sample size of 4 was used for degradable hydrogels with the exception of day 46 where a sample size was one for loaded acrylate system and a sample size of two for loaded thiol-norbornene systems.

Histology and Immunohistochemistry

At specified time points, constructs were fixed overnight in 4% paraformaldehyde, dehydrated, embedded in paraffin and sectioned. Sections (10μm) were stained with Safranin-O/Fast Green, which stains negatively charged sGAGs. For immunohistochemistry, sections were pretreated with chondroitinase-ABC (Sigma) for anti-aggrecan, hyaluronidase (Sigma) for anti-collagen II, anti-collagen VI and anti-C1,2C, or pepsin (Sigma) for anti-collagen I. Anti-collagen X sections were sequentially pretreated with protease (Sigma) then pepsin. Sections were permeabilized with Triton-X 100™, blocked with BSA, and treated with the appropriate antibody: anti-aggrecan (US Biologicals; 1:5), anti-collagen II (US Biologicals; 1:25), anti-collagen VI (Abcam; 1:25), anti-collagen I (Abcam; 1:50), anti-collagen X (Abcam; 1:50), or anti-C1,2C (IBEX; 1:100). Sections were treated with secondary antibodies: goat anti-mouse or goat anti-rabbit IgG labeled with AlexaFluor® 546 or 488 (Invitrogen; 1:200) and counterstained with DAPI. For each antibody, sections were stained at the same time to minimize batch-to-batch variations. Sections were imaged on a laser scanning confocal microscope (Zeiss LSM 5 Pascal), where laser, pinhole and objective settings were consistent among all images for each antibody. Semi-quantitative

analysis was performed using NIH ImageJ software with three images per hydrogel (n=4). Mean fluorescence intensity was normalized to the number of nuclei for each image.

Statistical Analysis

All quantitative data are expressed as mean with error bars representing standard deviation (mean(SD)). Data were compared using a student's t-test or three-way analyses of variance (ANOVA) with α of 0.05 and factors of culture time, hydrogel system (acrylate or thiol-norbornene), and loading condition (free swelling or loaded). Cell straining variance was analyzed using an F-test with α of 0.05. Significance was established for $p \leq 0.05$. P-values are presented on immunohistochemistry figures when below p=0.15.

Results

Characterization of Non-degradable Hydrogels

PEG hydrogels were formed under the same photoinitating conditions from either PEG diacrylate macromers or PEG tetranorbornene and PEG dithiol macromers as shown in Fig. 1. Macromer concentration prior to polymerization was adjusted such that the initial double bond concentration and the resulting tangent compressive modulus were similar for both systems. The initial double bond concentration was 28.0 mM for the acrylate system and 28.5mM for the thiol-norbornene system. The tangent compressive modulus for the chondrocyte-laden hydrogels was 31.8(3.1) kPa for the diacylate system and 33.7(1.9) kPa for the thiol-norbornene system.

Hydrogel Gelation and Affect on Chondrocytes

Photorheometry was used to characterize the evolution of gelation for the acrylate and thiol-norbornene reaction systems in the absence and presence of chondrocytes (Fig. 2a). The onset of gelation is determined by a sudden increase in G' and by the point at which G' and G'' cross (data not shown for G''). For the acrylate system, there was a delay in gelation, which began after 101(9)s in the absence of cells and 110(6)s in the presence of cells. For the thiol-norbornene system, the gel point occurred at 10(4)s and 9(4)s in the absence and presence of chondrocytes, which was significantly shorter than the acrylate system ($p<0.001$). For the acrylate system, the final shear storage modulus was 2090(670) Pa when cells were present and significantly higher ($p=0.009$) when cells were absent at 3840(430) Pa. For the thiol-norbornene system, the presence of cells did not significantly affect the final shear storage modulus, which was 1980(710) Pa with cells and 2270(640) Pa without cells. The data are summarized in Table 1.

Immediately after encapsulation, there was elevated intracellular ROS in chondrocytes encapsulated in the acrylate hydrogel (Fig. 2b). On the contrary, there was minimal intracellular ROS in the thiol-norbornene hydrogel (Fig. 2c). After 24 hours of encapsulation, cell viability based on a membrane integrity assay was similar in both acrylate and thiol-norbornene PEG hydrogels (Fig. 2d, e).

Cell Deformation in Mechanically Strained Hydrogels

Chondrocytes encapsulated in acrylate and thiol-norbornene PEG hydrogels had statistically similar diameter ratios, which were 1.010(0.062), 1.001(0.059), respectively (Fig. 3a, c, Table 1). Upon an application of 20% compressive strain to the hydrogels, the cell diameter ratio decreased from unity to 0.614(0.095) ($p<0.001$) within the acrylate hydrogel (Fig. 3b, Table 1) and to 0.637(0.076) ($p<0.001$) within the thiol-norbornene hydrogel (Fig. 3d, Table 1). Cells adopted an ellipsoid morphology as shown by the representative images in Fig. 3e, f. The variance in cell diameter ratio increased for both systems under 20% strain, but was significantly higher ($p=0.007$) in the acrylate hydrogels (variance of 0.0090) compared to the thiol-norbornene hydrogels (variance of 0.0057).

Tissue Formation in Non-degradable Hydrogels

Chondrocyte viability was maintained throughout 14 days of culture in the acrylate and thiol-norbornene PEG hydrogels under free swelling and dynamic loading culture conditions (data not shown). The tangent modulus measured under compression was affected by PEG hydrogel system (acrylate and thiol-norbornene) and loading condition, but not culture time ($p\leq0.004$; Table 2, Fig. 4). By day 14, thiol-norbornene hydrogels under dynamic loading had the highest tangent modulus, which was significantly greater than the free swelling condition ($p<0.001$). The tangent modulus of acrylate hydrogels was similar for free swelling and loaded conditions and by day 14 was lower than the thiol-norbornene PEG hydrogels under free swelling and loading ($p<0.05$).

Tissue content was analyzed by sGAG content in the constructs and by spatial deposition of sGAG and aggrecan (Fig. 5). PEG hydrogel system (acrylate versus thiol-norbornene) and culture time, but not loading, were significant factors impacting sGAG content ($p<0.001$) (Table 2 and Fig. 5a). Thiol-norbornene hydrogels had ~35% lower sGAG content per dry weight after 14 days when compared to the acrylate PEG hydrogels regardless of culture condition, with dry weight being ~20% higher for the thiol-ene system (Supplementary Fig. 1). SGAGs were distributed pericellularly and throughout the hydrogel in both hydrogel systems (Fig. 5c, e, g, i). There appeared to be more sGAG pericelluarly in the thiol-norbornene PEG hydrogels evidenced by the darker staining when compared to the acrylate PEG hydrogels. Aggrecan was limited to the pericellular region in both hydrogel systems (Fig. 5d, f, h, j) and appeared to be greater within thiol-norbornene PEG hydrogel compared to acrylate hydrogel, which is suggested by semi-quantitative analysis ($p=0.147$; Fig. 5b).

Tissue content was also analyzed by collagen content (Fig. 6, Fig. 7 and Table 2). PEG hydrogel system (acrylate versus thiol-norbornene) and culture time, but not loading were significant factors affecting total collagen content (Table 2). Total collagen content per dry weight at day 14 was 2.1–fold and 4.6–fold greater in the acrylate hydrogel under free swelling and loading, respectively, when compared to the respective thiol-norbornene hydrogels (Fig. 6, $p<0.05$). At day 14, there was 17.5% more total collagen in the acrylate hydrogels as a result of loading ($p=0.068$). In contrast, loading down-regulated the mean total collagen content by 46% in the thiol-norbornene hydrogels. To assess the type of collagen in the two hydrogel systems, immunohistochemistry was performed (Fig. 7). At day 14 under free swelling conditions, deposition of collagen types I and II was similar for

both hydrogel systems. However collagen type X was detected in the acrylate hydrogels, but only minimally in the thiol-norbornene hydrogels. Loading of the acrylate hydrogel did not have an affect on the type of collagen (I, II or X) deposited. Loading of the thiol-norbornene PEG hydrogel did not affect collagen types II or X, but appeared to reduce collagen type I ($p=0.141$). Under loading, thiol-norbornene hydrogels contained mostly collagen type II while the acrylate hydrogels had substantial amounts of collagen types I, II and X. Collagen type VI staining was similar for all hydrogels (Supplementary Fig. 3). Catabolic activity of collagen was assessed by probing for the presence of the C1,2C neoepitope. Under free swelling and loaded conditions, the presence of C1,2C was detected in both hydrogel systems, but to a much higher degree in acrylate PEG hydrogels ($p=0.008$). Loading did appear to elevate collagen degradation in the thiol-norbornene system, although not significantly. Select data are summarized in Table 1.

Tissue Formation in Degradable PEG

Hydrolytically labile ester linkages were incorporated into acrylate and thiol-norbornene PEG hydrogels to form degradable hydrogels (Fig. 8a, b). The macromer concentration prior to polymerization was adjusted such that the initial double bond concentration and the resulting tangent compressive modulus were similar for both systems. The initial double bond concentration was estimated to be 29.2 mM in the degradable acrylate hydrogel and 27.6 mM in the degradable thiol-norbornene hydrogel. The initial tangent compressive modulus of the cell-laden hydrogels was 47(2.5)kPa and 48.2(0.8)kPa for the acrylate and thiol-norbornene system, respectively. Hydrogel degradation was characterized by mass loss and determined to be on the timescale of the cell studies resulting in complete degradation by 18 days for the acrylate hydrogel and by 37 days for the thiol-norbornene hydrogel in the absence of cells (Fig. 8c). Chondrocytes remained viable throughout 46 days of culture (data not shown). Because hydrogel degradation occurred on different timescales, tissue quantity was normalized to cell number. Hydrogel system (acrylate versus thiol-norbornene) ($p=0.001$) and loading ($p=0.028$), but not culture time, were significant factors affecting sGAG content (Fig. 8d, Supplementary Fig. 4). At 46 days, sGAG content was 17.4–fold higher in the thiol-norbornene hydrogels conditions when compared to acrylate hydrogels, cultured under free swelling. Total collagen content was affected by culture time ($p<0.001$), but not by hydrogel system or loading (Table 2, Fig. 8e, Supplementary Fig. 4). Immunohistochemistry provided insight into the quality of the engineered tissue (Fig. 9), but is limited due to degradation of the hydrogels occurring during histological processing. Therefore, only information regarding the composition of the pericellular matrix was obtained. Deposition of collagen type II and aggrecan were present in both hydrogel systems. However, deposition of collagen types I and X appeared higher in acrylate hydrogels compared to the thiol-norbornene hydrogels.

Discussion

In this study, we demonstrate that polymerization mechanism and network structure have short- and long- term effects on chondrocytes encapsulated in PEG hydrogels. The main findings are as follows: (a) polymerization mechanism has an immediate effect on chondrocytes during encapsulation, indicating that the type of radical plays an important

role; (b) network structure alters cell deformation under a mechanical strain, suggesting that the local mechanical cues perceived by the encapsulated cells will be different; and (c) the hydrogel system (polymerization mechanism and network structure) affects the quantity and quality of the neo-cartilage formed, which is further accentuated under mechanical loading, suggesting that the PEG hydrogel system has long-term effects on the tissue engineering outcome.

To enable comparison between the two hydrogel systems, it was important to create cell-laden hydrogels with similar macroscopic properties. The theory of rubber elasticity relates bulk properties of crosslinked networks to the underlying microscopic structure of the material and states that the rubbery modulus scales with crosslink density and temperature [17, 38]. Therefore, by matching the modulus of the two hydrogel systems, the average crosslink density is matched. As crosslink density influences many of the properties important in a tissue engineering scaffold (e.g., mechanics, diffusion), this structural property provides a basis for comparing acrylate and thiol-norbornene PEG systems. However, it is important to recognize that there are inherent discrepancies in the network structure, which arise from differences in chain length and cyclization, as well as chemistry [27].

The polymerization behavior was markedly different between the thiol-norbornene step-growth system and the acrylate chain-growth system even though the photoinitiation reaction was similar. These differences are in large part attributed to differences in the reactivity with oxygen and polymerization-induced ROS (e.g., peroxy radicals). Since peroxy radicals do not readily initiate chain-growth polymerization of acrylates, a delay in the onset of polymerization is observed until dissolved oxygen is consumed [21]. This phenomenon can be seen in the rheometry data for the acrylate system. Contrarily, the thiol-norbornene polymerization proceeds rapidly in the presence of dissolved oxygen showing no delay in gelation. The latter occurs because ROS can abstract a hydrogen from a thiol enabling propagation to continue in the presence of oxygen [10]. Our findings are in agreement with other reports describing the polymerization behavior of these systems in the presence of oxygen [11, 39].

When cells were present during gelation, the polymerization behavior was unchanged for the thiol-norbornene system, but was impacted for the acrylate system. In the latter, the G'/G'' crossover point was delayed by ~9 seconds although not statistically significant. More notably, the final storage modulus was significantly reduced when cells were present. It is hypothesized that due to the high reactivity of acrylate-based radicals, cells act as chain transfer agents leading to early termination of the propagating radicals, which causes a decrease in crosslink density and hence modulus [17, 38]. The thiol-norbornene polymerization, however, does not appear to be affected by the presence of cells. In this system, others have reported high recovery of encapsulated proteins [39], suggesting that norbornene may preferentially propagate with the thiol macromers and minimally with cells and/or proteins. The idea that chondrocytes act as chain transfer agents in the acrylate system is further confirmed by our analysis of cell deformation where larger variations in cell deformation were observed. Heterogeneities in network structure of acrylate systems have been shown to occur at the nanometer length scale [26]. However for large variations

to occur in cell deformation, network heterogeneities must exist at a much larger length scale (e.g., micron scale). We therefore hypothesize that chondrocytes alter the local polymerization leading to network heterogeneities surrounding each cell which is further accentuated because primary chondrocytes isolated from full depth cartilage represent a heterogeneous population of cells [40]. In the thiol-norbornene system where cells appear not to affect the polymerization, cell deformation was more uniform further supporting this hypothesis.

With cells influencing the polymerization for the acrylate system, questions arise as to whether cells are subsequently affected. While chondrocyte viability was similar, a large accumulation of intracellular ROS was observed in chondrocytes immediately after encapsulation in the acrylate, but not the thiol-norbornene system. Similar findings were reported for encapsulated β-cells, which are known to be sensitive to radicals, showing reduced viability and function in acrylate hydrogels compared to thiol-norbornene hydrogels [41]. During polymerization, initiator radicals, polymerization induced ROS, and propagating radicals can attack cells. Given that the photoinitaiting conditions are the same in both systems and that not all photoinitiator molecules are consumed with 10 minutes of light exposure [15], the initiator radicals are likely not responsible for the large increase in ROS. Since ROS cannot participate in the polymerization of the acrylate system as it can in the thiol-norbornene system [11, 21], ROS may have a higher propensity to react with cells in the acrylate system. Moreover, there is evidence in the literature to suggest that propagating acrylate-based radicals are more reactive than the norbornene radicals, which may lead to damaging reactions with proteins and/or lipids in the cell membrane [39]. Previous studies have confirmed that lipid peroxidation of the cell membrane occurs in chondrocytes during encapsulation with similar PEG acrylate systems [42], which can lead to intracellular ROS generation [43]. We therefore hypothesize that the polymerization induced ROS and propagating acrylate-based radicals attack the cells during encapsulation leading to upregulation of intracellular ROS in the acrylate system.

Given that the encapsulation process for acrylate and thiol-norbornene systems differentially influence chondrocytes, questions arise as to whether these differences have long term effects on the cells. Indeed, our findings confirm that under free swelling culture and for non-degrading hydrogels the type of neocartilage formed in the two hydrogel systems is distinctly different. The tissue (sGAG and total collagen) quantity was higher in the acrylate system, however the quality of the tissue in the thiol-norbornene system better resembled hyaline articular cartilage. There appeared to be more aggrecan, the large cartilage proteoglycan comprised of sGAGs, within thiol-norbornene system despite sGAG quantity being higher in acrylate system. The higher total collagen content in the acrylate system appeared to be due to non-hyaline cartilage collagens, namely the presence of collagen type X, since collagen types I and II appeared similar for both systems. Catabolic activity was also elevated in the acrylate system, evidenced by positive staining for the MMP cleaved collagen neoepitope (C1,2C), which was minimal in the thiol-norbornene system. The differences in intracellular ROS during encapsulation may explain the differences observed in the type of tissue produced in the two systems. Elevated intracellular ROS have been directly implicated in upregulation of catabolic activity [24, 25] (e.g., up-regulating the expression of genes coding for matrix metalloproteinase (MMP) [44] and activating MMPs

[25]), inducing hypertrophy in cartilage (e.g., collagen X production) [45] and mediating osteoarthritis [48, 49]. Overall our results indicate that the neo-cartilage produced in thiol-norbornene systems appears more hyaline-like while that produced in acrylate system appears more hypertrophic-like; a finding that is attributed to the elevated intracellular ROS levels induced during cell encapsulation in the acrylate polymerization system. However, additional experiments are needed to confirm this hypothesis.

Dynamic compressive loading has been identified as an important signal for chondrocytes and maintenance of cartilage [46]. In this study, the application of dynamic compressive loading differentially regulated the quantity and type of tissue produced in the acrylate and thiol-norbornene systems. Dynamic loading had no affect on sGAG content or aggrecan deposition, but did affect total collagen content and collagen type. Loading enhanced total collagen content in the acrylate system, but lowered it in the thiol-norbornene system. Interestingly, loading improved the quality of the neocartilage in thiol-norbornene system by reducing collagen type I deposition without appearing to effect collagen type II. Despite having lower sGAG and lower total collagen contents, mechanically loaded thiol-norbornene hydrogels had the highest compressive modulus, suggesting that loading may have improved the organization and/or quality of the ECM molecules [47]. While the exact mechanism remains to be elucidated, we hypothesize that an improved state of the cell after encapsulation and a more homogeneous strain field applied to the encapsulated cells contributed to the improved quality of neo-cartilage, leading to hyaline-like cartilage composed of primarily aggrecan and collagen type II and minimal collagen types I and X in the thiol-ene system.

To determine whether these findings translate to hydrogel systems more applicable for tissue engineering, degradable crosslinks were incorporated into the hydrogels. The polymerization proceeds in the same manner as in the non-degradable systems, and therefore, it is not surprising that the degradable systems produced a similar type of neo-cartilage as to the non-degradable systems. The degradable acrylate system resulted in a hypertrophic-like neocartilage evidenced by positive staining for aggrecan and collagen types I, II and X, while degradable thiol-norbornene system produced hyaline-like neocartilage evidenced by staining primarily for aggrecan and collagen type II with minimal staining for collagen types I and X. However under dynamic loading, the quality of tissue (i.e., the types of collagen) did not appear to change. With hydrogel degradation, mechanical properties decrease leading to evolving mechanical cues sensed by the cells. As cells form a stiff pericellular matrix in tandem with decreasing hydrogel mechanics, the cells will no longer sense the mechanical strains and therefore may be less responsive to loading [18]. This observation may explain why loading had less of an effect on the quality of the tissue when compared to the non-degrading hydrogels. In addition, degradation leads to increases in mesh size and therefore enhanced diffusion of ECM molecules, which is further accentuated by loading. This observation may explain the reduced sGAG content under loading for both degradable thiol-norbornene and acrylate systems. Finally, sGAG and total collagen contents in the hydrogel continued to increase in the degradable thiol-norbornene system over long-term cultures, which was not observed in the acrylate systems, indicating that thiol-norbornene degradable systems led to greater overall ECM accumulation per chondrocyte. Overall, these results with the degradable hydrogels further support the finding that the neo-cartilage

produced in thiol-norbornene systems is more hyaline-like than that produced in the acrylate systems.

Conclusions

This study demonstrates that the encapsulation process occurring over a ten minute period can have a dramatic effect on the type of tissue produced by chondrocytes when encapsulated in hydrogels formed from acrylate and thiol-nobornene systems. Given that the bulk mechanical properties are similar for these two hydrogels systems, our findings point towards the encapsulation process as having a long term effect on the quality of the engineered tissue. Overall, the acrylate system leads to an encapsulation environment that results in elevated intracellular ROS and neo-tissue that resembles hypertrophic cartilage. On the other hand, the thiol-norbornene system leads to a milder encapsulation environment resulting in minimal intracellular ROS and after several weeks the deposition of a neo-tissue that better resembles hyaline cartilage, especially under mechanical loading. Our findings indicate that the choice of polymerization mechanism and hydrogel network structure are essential design considerations, which can have long-term effects on the tissue engineering outcome.

Supplementary Material

Refer to Web version on PubMed Central for supplementary material.

Acknowledgments

The authors are grateful to a Department of Education Graduate Assistantships in Areas of National Need (GAANN) Fellowship and University of Colorado-National Institute of Standards and Technology (CU-NIST) Material Science and Engineering Fellowship to JJR; as well as the National Institute of Health (R21AR061011).

References

1. Ma, PX.; Elisseeff, JH. Scaffolding in tissue engineering. Boca Raton: Taylor&Francis; 2005.
2. Temenoff JS, Park H, Jabbari E, Conway DE, Sheffield TL, Ambrose CG, et al. Thermally cross-linked oligo(poly(ethylene glycol) fumarate) hydrogels support osteogenic differentiation of encapsulated marrow stromal cells in vitro. Biomacromolecules. 2004
3. Jin, R.; Dijkstra, PJ. Hydrogels for tissue engineering applications. In: Park, K.; Okano, T.; Ottenbrite, RM., editors. Biomedical applications of hydrogels handbook. New York: Springer; 2010.
4. Elisseeff J, Anseth K, Sims D, McIntosh W, Randolph M, Langer R. Transdermal photopolymerization for minimally invasive implantation. Proc Natl Acad Sci USA. 1999; 96(6): 3104–3107. [PubMed: 10077644]
5. Bryant, SJ.; Anseth, KS. Photopolymerization of hydrogel scaffolds. In: Ma, PX.; Elisseeff, JH., editors. Scaffolding in tissue engineering. Boca Raton: Taylor&Francis; 2005.
6. Smeds KA, Grinstaff MW. Photocrosslinkable polysaccharides for in situ hydrogel formation. J Biomed Mater Res. 2001; 54(1):115–121. [PubMed: 11077410]
7. Steinmetz NJ, Bryant SJ. Chondroitin sulfate and dynamic loading alter chondrogenesis of human MSCs in PEG hydrogels. Biotechnol Bioeng. 2012; 109(10):2671–2682. [PubMed: 22511184]
8. Bryant SJ, Arthur JA, Anseth KS. Incorporation of tissue-specific molecules alters chondrocyte metabolism and gene expression in photocrosslinked hydrogels. Acta Biomater. 2005; 1(2):243–252. [PubMed: 16701801]

9. Li Q, Williams CG, Sun DDN, Wang J, Leong K, Elisseeff JH. Photocrosslinkable polysaccharides based on chondroitin sulfate. J Biomed Mater Res A. 2004; 68(1):28–33. [PubMed: 14661246]
10. Cramer NB, Bowman CN. Kinetics of thiol-ene and thiol-acrylate photopolymerizations with real-time Fourier transform infrared. J Polym Sci A Polym Chem. 2001; 39(19):3311–3319.
11. Fairbanks B, Schwartz MP, Halevi AE, Nuttelman CR, Bowman CN, Anseth KS. A versatile synthetic extracellular matrix mimic via thiol-norbornene photopolymerization. Adv Mater. 2009; 21:5005–5010. [PubMed: 25377720]
12. Bryant SJ, Anseth KS, Chowdhury T, Lee DA, Bader DL. Crosslinking density influences chondrocyte metabolism in dynamically loaded photocrosslinked poly(ethylene glycol) hydrogels. Ann Biomed Eng. 2004; 32(3):407–17. [PubMed: 15095815]
13. Sawhney AS, Pathak CP, Hubbell JA. Bioerodible hydrogels based on photopolymerized poly(ethylene glycol)-co-poly(alpha-hydroxy acid) diacrylate macromers. Macromolecules. 1993; 26(4):581–587.
14. Martens PJ, Bryant SJ, Anseth KS. Tailoring the degradation of hydrogels formed from multivinyl poly(ethylene glycol) and poly(vinyl alcohol) macromers for cartilage tissue engineering. Biomacromolecules. 2003; 4(2):283–292. [PubMed: 12625723]
15. Fairbanks BD, Schwartz MP, Bowman CN, Anseth KS. Photoinitiated polymerization of PEG-diacrylate with lithium phenyl-2,4,6-trimethylbenzoylphosphinate: polymerization rate and cytocompatibility. Biomaterials. 2009; 30(35):6702–6707. [PubMed: 19783300]
16. Bryant SJ, Nuttelman CR, Anseth KS. Cytocompatibility of ultraviolet and visible light photoinitiating systems on cultured NIH/3T3 fibroblasts in vitro. J Biomat Sci Polym Ed. 2000; 11(5):439–457.
17. Kloxin AM, Kloxin CJ, Bowman CN, Anseth KS. Mechanical properties of cellularly responsive hydrogels and their experimental determination. Adv Mater. 2010; 22(31):3484–3494. [PubMed: 20473984]
18. Bryant SJ, Anseth KS, Lee DA, Bader DL. Crosslinking density influences the morphology of chondrocytes photoencapsulated in PEG hydrogels during the application of compressive strain. J Orthop Res. 2004; 22(5):1143–1149. [PubMed: 15304291]
19. O'Brien AK, Bowman CN. Impact of oxygen on photopolymerization kinetics and polymer structure. Macromolecules. 2006; 39(7):2501–2506.
20. Ruiz CSB, Machado LDB, Volponi JE, Pino ES. Oxygen inhibition and coating thickness effects on UV radiation curing of weatherfast clearcoats studied by Photo-DSC. J Therm Anal Calorim. 2004; 75(2):507–512.
21. O'Brien AK, Cramer NB, Bowman CN. Oxygen inhibition in thiol–acrylate photopolymerizations. J Polym Sci A Polym Chem. 2005; 44:2007–2014.
22. Machlin LJ, Bendich A. Free-radical tissue damage: protective role of antioxidant nutrients. FASEB J. 1987; 1(6):441–445. [PubMed: 3315807]
23. Carlo MD, Loeser RF. Increased oxidative stress with aging reduces chondrocyte survival: correlation with intracellular glutathione levels. Arthritis Rheum. 2003; 48(12):3419–3430. [PubMed: 14673993]
24. Borsiczky B, Szabo Z, Jaberansari MT, Mack PP, Roth E. Activated PMNs lead to oxidative stress on chondrocytes: a study of swine knees. Acta Orthop Scand. 2003; 74(2):190–195. [PubMed: 12807328]
25. Murrell GA, Jang D, Williams RJ. Nitric oxide activates metalloprotease enzymes in articular cartilage. Biochem Biophys Res Commun. 1995; 206(1):15–21. [PubMed: 7529496]
26. Lin-Gibson S, Jones RL, Washburn NR, Horkay F. Structure-property relationships of photopolymerizable poly(ethylene glycol) dimethacrylate hydrogels. Macromolecules. 2005; 38:2897–2902.
27. Tibbitt MW, Kloxin AM, Sawicki LA, Anseth KS. Mechanical properties and degradation of chain and step polymerized photodegradable hydrogels. Macromolecules. 2013; 46(7):2785–2792.
28. Cruise GM, Scharp DS, Hubbell JA. Characterization of permeability and network structure of interfacially photopolymerized poly(ethylene glycol) diacrylate hydrogels. Biomaterials. 1998; 19(14):1287–1294. [PubMed: 9720892]

29. Bryant SJ, Bender RJ, Durand KL, Anseth KS. Encapsulating chondrocytes in degrading PEG hydrogels with high modulus: engineering gel structural changes to facilitate cartilaginous tissue production. Biotechnol Bioeng. 2004; 86(7):747–755. [PubMed: 15162450]
30. Villanueva I, Weigel CA, Bryant SJ. Cell-matrix interactions and dynamic mechanical loading influence chondrocyte gene expression and bioactivity in PEG-RGD hydrogels. Acta Biomater. 2009; 5(8):2832–2846. [PubMed: 19508905]
31. Knight MM, Ghori SA, Lee DA, Bader DL. Measurement of the deformation of isolated chondrocytes in agarose subjected to cyclic compression. Med Eng Phys. 1998; 20(9):684–688. [PubMed: 10098613]
32. Nicodemus GD, Bryant SJ. The role of hydrogel structure and dynamic loading on chondrocyte gene expression and matrix formation. J Biomech. 2008; 41(7):1528–1536. [PubMed: 18417139]
33. Chiou BS, English RJ, Khan SA. Rheology and photo-cross-linking of thiol-ene polymers. Macromolecules. 1996; 29(16):5368–5374.
34. Kim YJ, Sah RL, Doong JY, Grodzinsky AJ. Fluorometric assay of DNA in cartilage explants using Hoechst 33258. Anal Biochem. 1988; 174(1):168–176. [PubMed: 2464289]
35. Farndale RW, Buttle DJ, Barrett AJ. Improved quantitation and discrimination of sulphated glycosaminoglycans by use of dimethylmethylene blue. Biochim Biophys Acta. 1986; 883(2):173–177. [PubMed: 3091074]
36. Woessner JF. Determination of hydroxyproline in tissue and protein samples containing small proportions of this imino acid. Arch Biochem Biophys. 1961; 93(2):440–447. [PubMed: 13786180]
37. Hollander AP, Heathfield TF, Webber C, Iwata Y, Bourne R, Rorabeck C, et al. Increased damage to type II collagen in osteoarthritic articular cartilage detected by a new immunoassay. J Clin Invest. 1994; 93(4):1722–1732. [PubMed: 7512992]
38. Flory PJRR. Statistical mechanics of crosslinked polymer networks. I. Rubberlike elasticity. J Chem Phys. 1943; 11(11):512–520.
39. McCall JD, Anseth KS. Thiol-ene photopolymerizations provide a facile method to encapsulate proteins and maintain their bioactivity. Biomacromolecules. 2012; 13(8):2410–2417. [PubMed: 22741550]
40. Athanasiou, KA.; Darling, EM.; Hu, JC. Articular cartilage tissue engineering. San Rafael, Calif: Morgan & Claypool Publishers; 2009.
41. Lin CC, Raza A, Shih H. PEG hydrogels formed by thiol-ene photo-click chemistry and their effect on the formation and recovery of insulin-secreting cell spheroids. Biomaterials. 2011; 32(36): 9685–9695. [PubMed: 21924490]
42. Farnsworth N, Bensard C, Bryant SJ. The role of the PCM in reducing oxidative stress induced by radical initiated photoencapsulation of chondrocytes in poly(ethylene glycol) hydrogels. Osteoarthritis Cartilage. 2012; 20(11):1326–1335. [PubMed: 22796510]
43. Sen S, Chakraborty R, Sridhar C, Reddy YSR, De B. Free radicals, antioxidants, diseases and phytomedicines: current status and future prospect. Int J Pharm Sci Rev Res. 2010; 3(1):91–100.
44. Sasaki K, Hattori T, Fujisawa T, Takahashi K, Inoue H, Takigawa M. Nitric oxide mediates interleukin-1-induced gene expression of matrix metalloproteinases and basic fibroblast growth factor in cultured rabbit articular chondrocytes. J Biochem. 1998; 123(3):431–439. [PubMed: 9538225]
45. Morita K, Miyamoto T, Fujita N, Kubota Y, Ito K, Takubo K, et al. Reactive oxygen species induce chondrocyte hypertrophy in endochondral ossification. J Exp Med. 2007; 204(7):1613–1623. [PubMed: 17576777]
46. Sah RL, Kim YJ, Doong JY, Grodzinsky AJ, Plaas AH, Sandy JD. Biosynthetic response of cartilage explants to dynamic compression. J Orthopaed Res. 1989; 7(5):619–636.
47. Lorenz H, Richter W. Osteoarthritis: cellular and molecular changes in degenerating cartilage. Prog Histochem Cytochem. 2006; 40(3):135–163. [PubMed: 16759941]

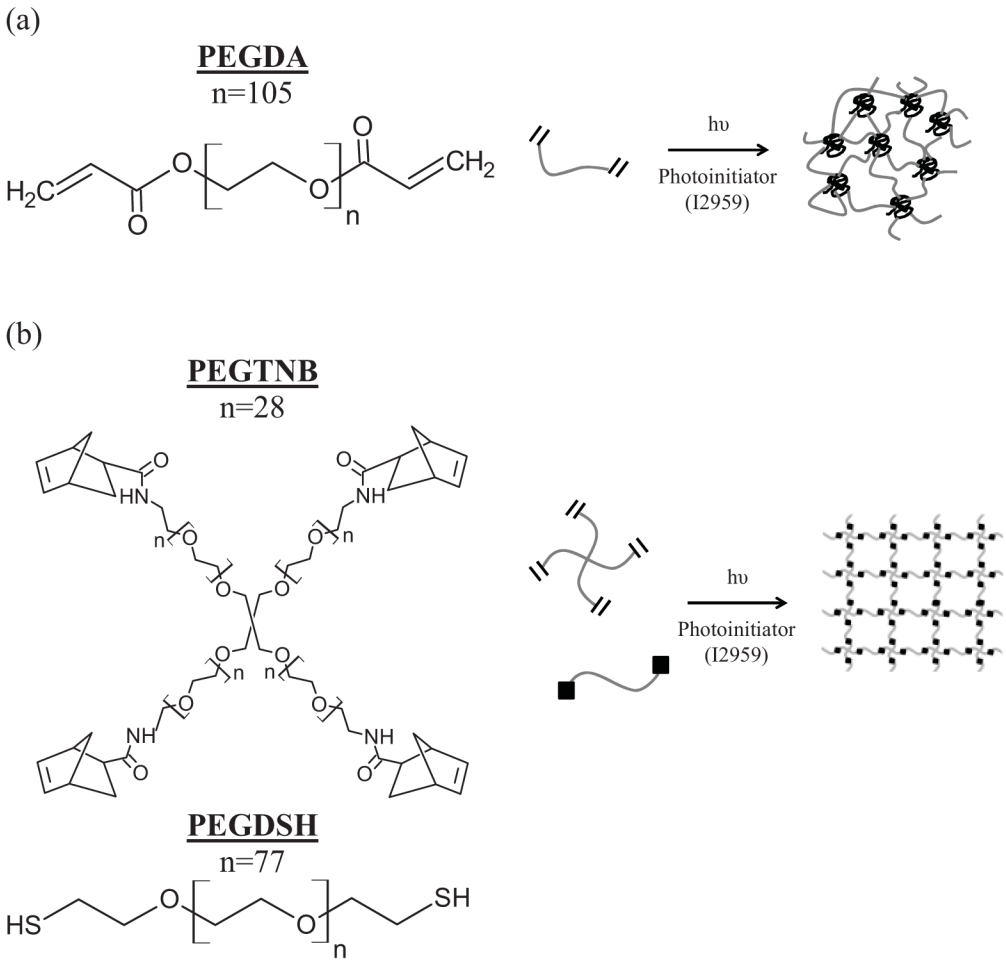

Figure 1.

Schematic of non-degradable poly(ethylene glycol) hydrogels formed from free radical photopolymerization of (a) chain-growth polymerization of poly(ethylene glycol) diacrylate (PEGDA) macromers and of (b) step-growth polymerization of poly(ethylene glycol) tetranorbornene (PEGTNB) and poly(ethylene glycol) dithiol (PEGDSH) macromers.

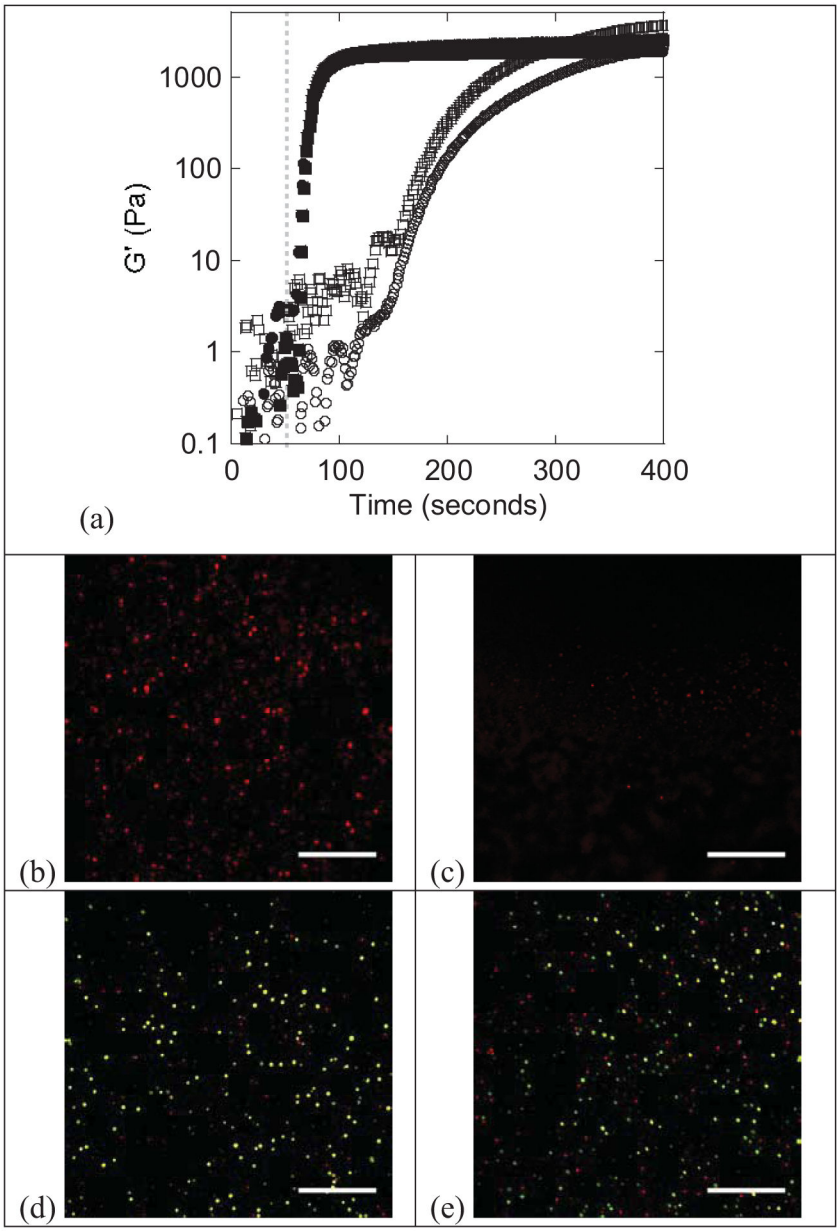

Figure 2.

(a) Representative plots of shear modulus (G′) as a function of time during photopolymerization of chain-growth acrylate (open) and step-growth thiol-norbornene (solid) hydrogel systems in the absence (squares) and presence (circles) of chondrocytes. The light was turned on at 60 seconds indicated by the gray dashed line. Representative confocal microscopy images of intracellular ROS (red) immediately following chondrocyte encapsulation in chain-growth acrylate hydrogels (b) and step-growth thiol-norbornene hydrogels (c). Representative confocal microscopy images of chondrocyte viability twenty-four hours post encapsulation in chain-growth acrylate hydrogels (d) and step-growth thiol-norbornene hydrogels (e). Live cells fluoresce green and dead cells fluoresce red. Scale bars represent 200 μm.

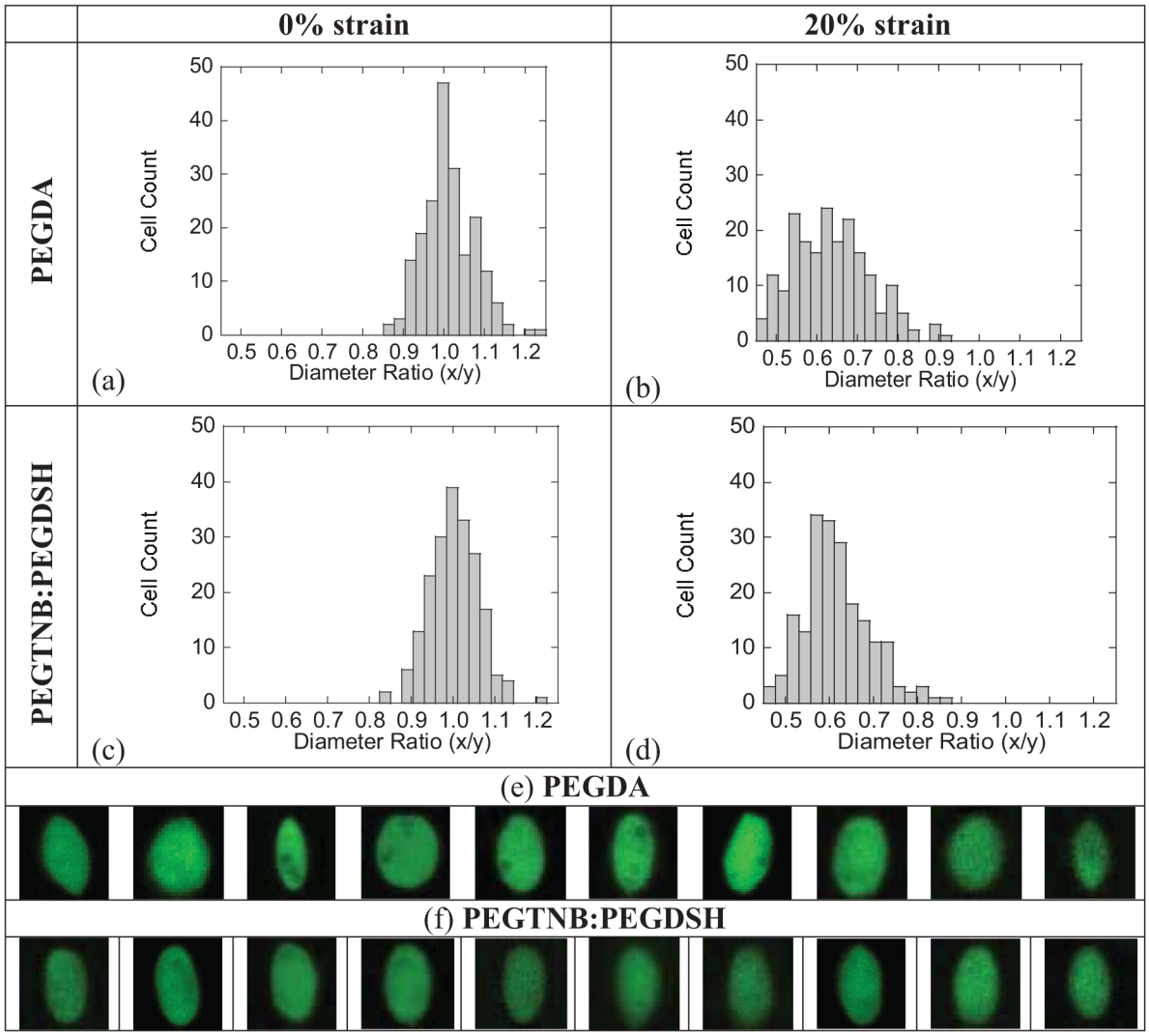

Figure 3.

Histograms of diameter ratio for chondrocytes encapsulated in chain-growth acrylate hydrogels and in step-growth thiol-norbornene hydrogels and subjected to no strain (a, c) or a 20% gross strain applied to the hydrogel (b, d). Diameter ratio (x/y) is defined as the cell diameter parallel to the applied strain (x) divided by the cell diameter perpendicular to the applied strain (y). Diameter ratios represent 4 different hydrogel samples and 50 cells per hydrogel. A selection of representative images of chondrocytes stained with calcein AM, which stains the cytosol of live cells green, in acrylate and thiol-nobornene hydrogels subjected to 20% gross strain (e, f).

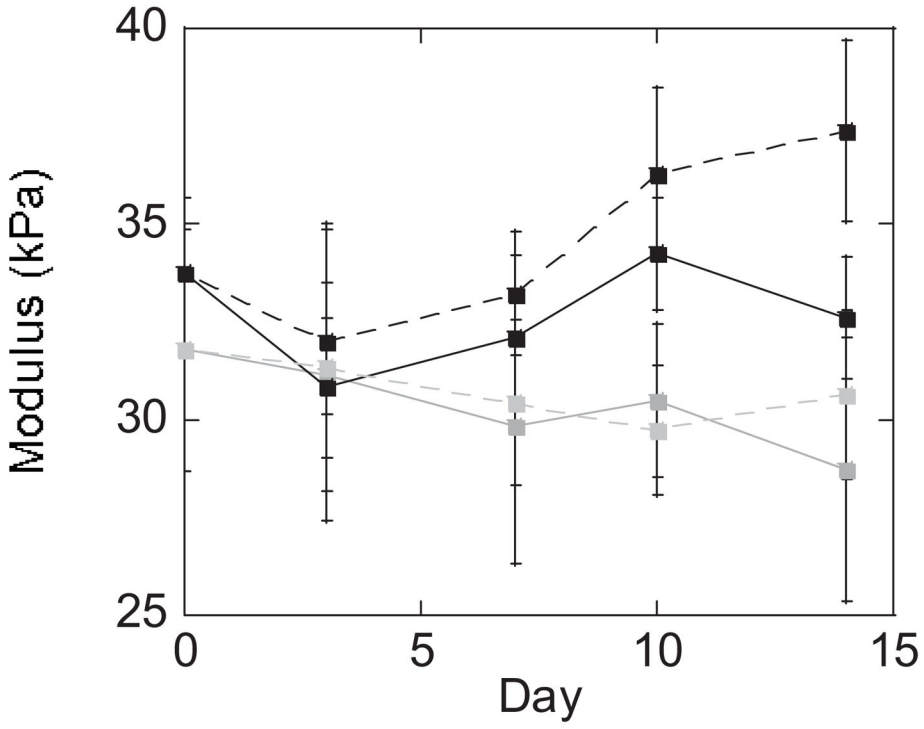

Figure 4.

Tangent modulus in unconfined compression for non-degradable chain-growth acrylate hydrogels (gray) and step-growth thiol-norbornene hydrogels (black) cultured up to 14 days under free swelling (solid lines) and dynamic loading (dashed lines) conditions. Data are represented as mean(SD) (n=8).

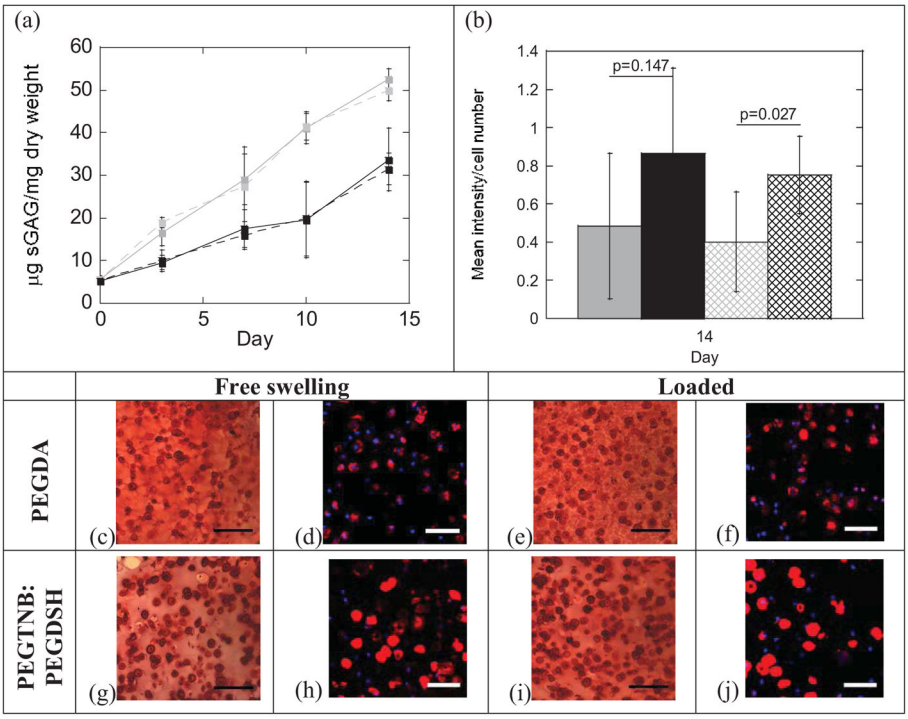

Figure 5.

Sulfated GAG (sGAG) production and aggrecan deposition in non-degradable chain-growth acrylate hydrogels and step-growth thiol-norbornene hydrogels. SGAG content (μg/dry construct weight) as a function of culture time for acrylate (gray) and thiol-norbornene (black) hydrogels under free swelling (solid lines) and dynamic loading (dashed lines) conditions (n=8) (a). Semi-quantitative assessment of aggrecan deposition for acrylate (gray) and thiol-norbornene (black) hydrogels under free swelling (solid bars) and dynamic loading (striped bars) conditions (n=4) (b). Representative images of sGAG (red) deposition by Safranin-O/Fast Green (c, e, g, i) and of aggrecan (red) deposition by immunohistochemistry (d, f, h, j) for acrylate and thiol-norbornene hydrogels after 14 days of free swelling or dynamic loading conditions. Nuclei were counterstained by hematoxylin (purple) (c, e, g, i) or DAPI (blue) (d, f, h, j). Images were acquired by optical microscopy (c, e, g, i) and laser scanning confocal microscopy (d, f, h, j). Scale bars represent 100 μm (c, e, g, i) and 50 μm (d, f, h, j). Data are represented as mean(SD).

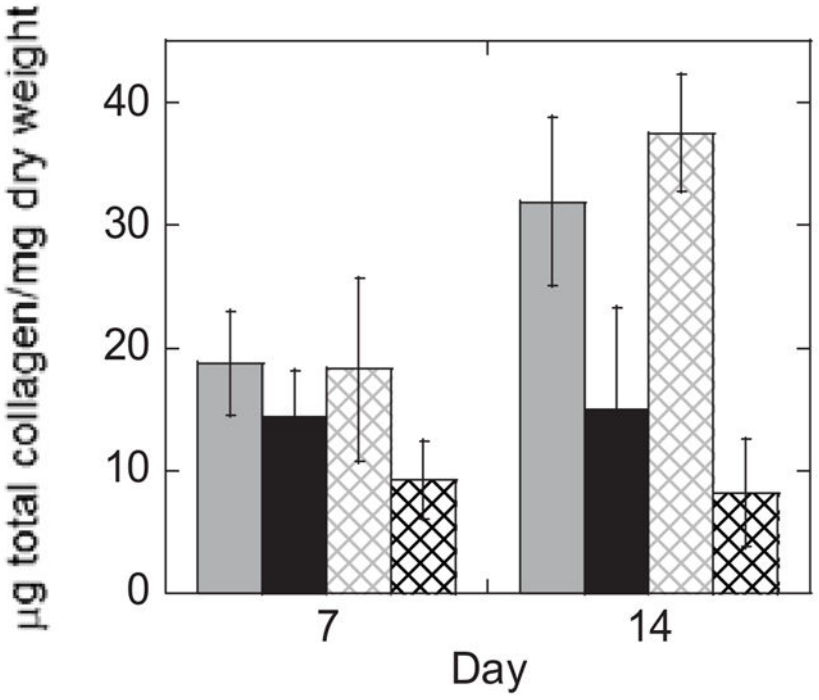

Figure 6.

Total collagen content (µg/dry construct weight) as a function of culture time for acrylate (gray) and thiol-norbornene (black) hydrogels under free swelling (solid lines) and dynamic loading (dashed lines) conditions. Data are represented as mean(SD) (n=8).

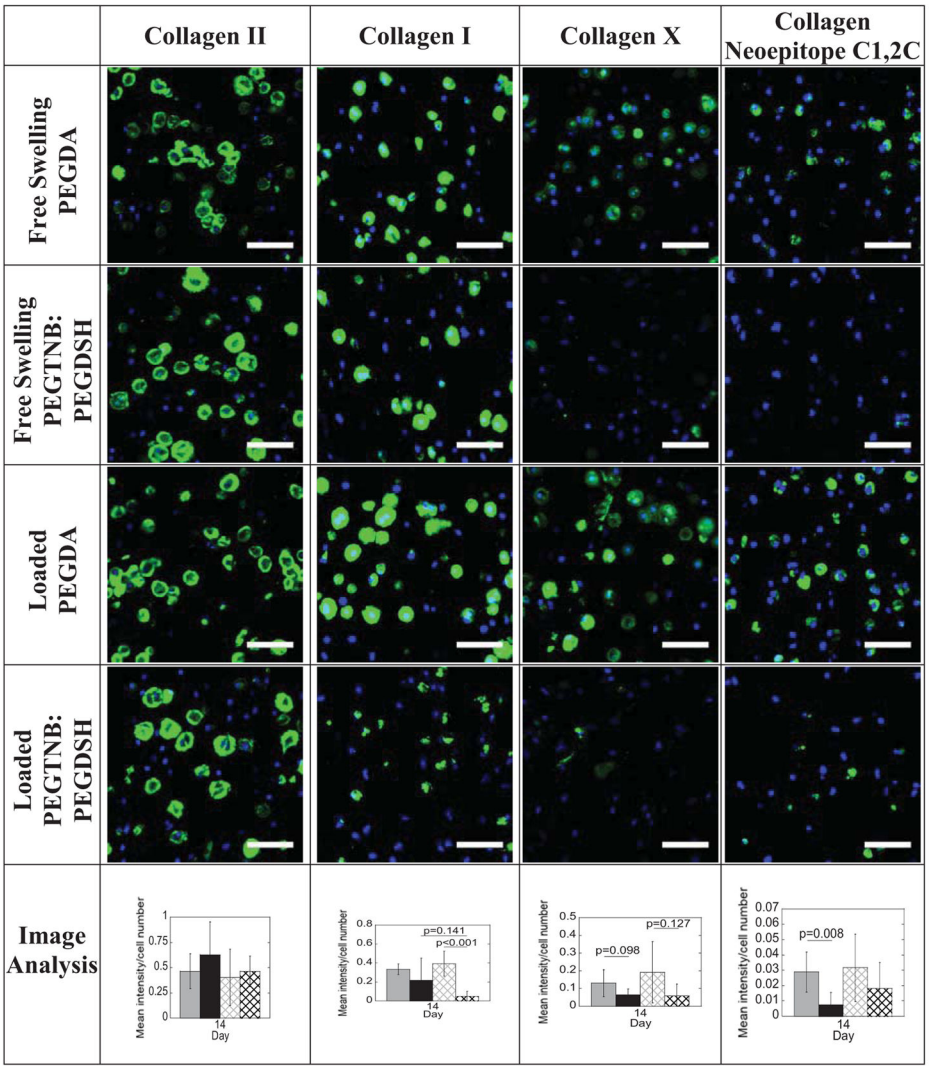

Figure 7.

Representative confocal microscopy images of collagen deposition by immunohistochemistry in non-degradable acrylate and thiol-norbornene hydrogels after 14 days of culture under free swelling or dynamic loaded conditions. Sections were stained using antibodies against collagen II, I, X, and C1,2C (green) and counterstained using DAPI for cell nuclei (blue). Scale bars represent 50 μm. Semi-quantitative image analysis was performed for acrylate (gray) and thiol-norbornene (black) hydrogels under free swelling (solid bars) or dynamic loaded (striped bars) conditions. Data are presented as mean(SD) (n=4).

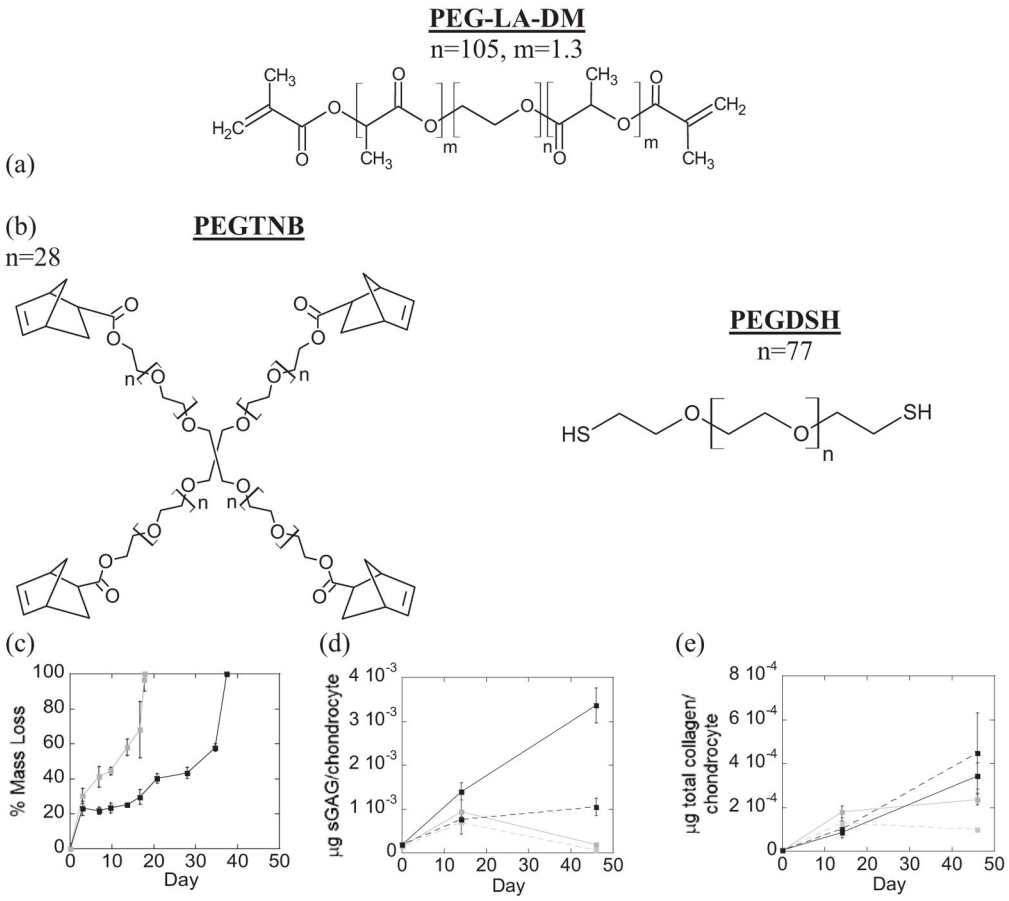

Figure 8.

Schematic of degrading hydrogels formed from free radical photopolymerization of (a) oligo(lactic acid)-b-PEG-b-oligo(lactic acid) diacrylate (PEG-LA-DA) macromers by chain-growth and (b) poly(ethylene glycol) tetranorbornene (degPEGTNB) and poly(ethylene glycol) dithiol (PEGDSH) macromers by step-growth. Mass loss as a function of time for the acrylate (gray) and thiol-nobornene (black) hydrogels in chondrocyte media (c). Matrix content (sGAG/chondrocyte (d) and total collagen/chondrocyte (e)) of chondrocyte-laden acrylate (gray) and thiol-norbornene (black) degradable hydrogels cultured up to 46 days under free swelling (solid lines) and dynamic loading (dashed lines) conditions. Data are represented as mean(SD) (n=4, except day 46 loaded for PEGDA n=1 and PEGTNB:PEGDSH n=2).

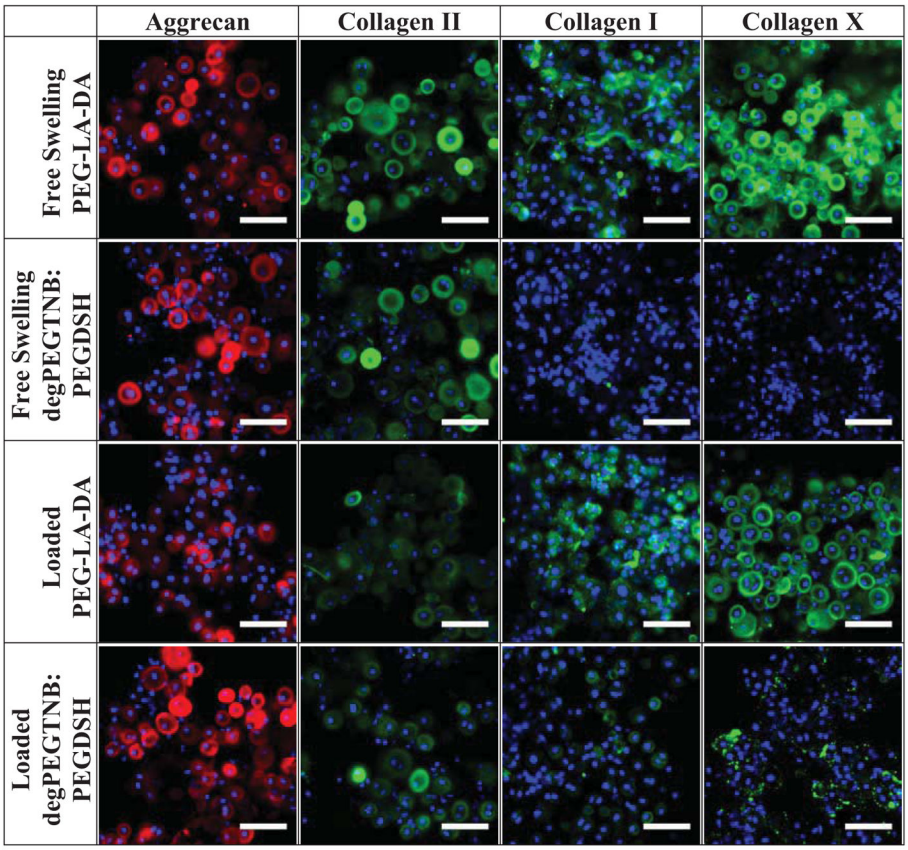

Figure 9.

Representative confocal microscopy images of matrix deposition by chondrocytes encapsulated in degradable acrylate and thiol-norbornene hydrogels after 14 days of culture. Sections were stained using antibodies against aggrecan (red) or collagen II, I, or X (green) and counterstained with DAPI for cell nuclei (blue). Scale bars represent 50 μm.

Biomaterials. Author manuscript; available in PMC 2015 July 15.

Table 1

Select data summarizing key differences between acrylate-based and thiol-ene PEG hydrogel systems

			Initial Characterization of Hydrogels[1]			Tissue Production[2]							
PEG Hydrogel System	***Culture Condition***	***Presence of Cells***	**Gelation Time (sec)**	**Shear Storage Modulus (Pa)**	**Cell Deformation (cell diameter ratio)**	**Tangent Modulus (kPa)**	**sGAG (μg)/mg dw[3]**	**Total Collagen (μg)/mg dw[3]**	**Aggrecan**	**Collagen I**	**Collagen II**	**Collagen VI**	**Collagen X**
Acrylate	*Free Swelling*	*No*	101(9)	3840(430)	--	--	--	--	--	--	--	--	--
		Yes	110(6)	2090(670)	1.010(0.062)	28.7(1.2)	52.5(0.9)	31.9(2.4)	**	***	***	**	**
	Loaded[4]	*Yes*	--	--	0.614(0.095)	30.6(0.8)	50.0(0.9)	37.5(1.7)	**	***	***	**	**
Thiol-ene	*Free Swelling*	*No*	10(4)	2270(640)	--	--	--	--	--	--	--	--	--
		Yes	9(4)	1980(710)	1.001(0.059)	32.6(0.6)	33.7(2.6)	15.0(2.9)	***	***	***	**	*
	Loaded[4]	*Yes*	--	--	0.637(0.076)	37.4(0.8)	31.5(1.3)	8.13(1.5)	***	*	***	**	*

[1,2]Data presented as mean(standard deviation).

[2]After 14 days of culture in non-degrading hydrogels, where abundance of ECM is denoted by *, **, or *** to indicate minimal staining, moderate staining, or intense staining based on immunohistochemistry images.

[3]dw is construct dry weight.

[4]Loaded describes static strain (20%) for cell deformation experiments and dynamic compressive loading (1 Hz, 10% amplitude strain) for tissue production.

Table 2

Three-way ANOVA was performed to evaluate the impact of culture time, PEG hydrogel system, and loading condition for (a) Figure 4, (b) Figure 5a, (c) Figure 6, (d) Figure 8d, and (e) Figure 8e.

	ANOVA Factors		
	Culture time	**Hydrogel system (acrylate or thiol- norbornene PEG)**	**Loading condition (free swelling or loaded)**
(a) Non-degradable PEG Hydrogel: Tangent modulus	p=0.114	p<0.001	p=0.004
(b) Non-degradable PEG Hydrogel: μg sGAG/mg dry weight	p<0.001	p<0.001	p=0.610
(c) Non-degradable PEG Hydrogel: μg collagen/mg dry weight	p<0.001	p<0.001	p=0.350
(d) Degradable PEG Hydrogel: μg sGAG/chondrocyte	p=0.304	p=0.001	p=0.028
(e) Degradable PEG Hydrogel: μg collagen/chondrocyte	p<0.001	p=0.296	p=0.910